ОБЪЕДИНЕННЫЙ
ИНСТИТУТ
ЯДЕРНЫХ
ИССЛЕДОВАНИЙ

Дубна

E14-98-119

T.N.Mamedov, I.L.Chaplygin, V.N.Duginov,
V.N.Gorelkin[1], D.Herlach[2], J.Major[3], A.V.Stoykov,
M.Schefzik[3], U.Zimmermann[2]

INVESTIGATION OF ACCEPTOR CENTERS IN SEMICONDUCTORS WITH DIAMOND CRYSTAL STRUCTURE BY THE $\mu^{-}SR$-METHOD

Submitted to «Письма в ЖЭТФ»

[1]Moscow Institute of Physics and Technology, 141700 Dolgoprudny, Moscow Region, Russia
[2]Paul Scherrer Institut, CH-5232 Villigen PSI, Switzerland
[3]Max-Planck-Institut für Metallforschung, D-70569 Stuttgart, Germany

1998

Introduction

The relaxation and precession frequency shift of negative muon spin in n- and p-type silicon at temperatures below 30 K were recently observed [1–3]. Muon spin relaxation in diamagnetic silicon was explained by paramagnetism of the electron shell of the muonic atom formed as a result of negative muon capture by an atom of silicon. Since the radius of the muon orbit in the 1S-state is 207 times smaller than that of the K-electron, the muon screens a unit of the nuclear charge from electrons of the atom shell. Thus in monoatomic matter the muonic atom imitates an impurity atom of the preceding element of the periodic table. In the case of semiconducting crystals it can be considered as an acceptor impurity atom. Investigation of negative muon polarization in semiconductors allows one to obtain information on the interaction of a solitary acceptor center with matter.

Contrary to donor impurities, behaviour of acceptors in semiconductors with diamond crystal structure (silicon, germanium, diamond) is studied incompletely as the application of traditional methods (EPR, ENDOR, etc.) used to study shallow acceptor centers is limited by a high spin-lattice relaxation rate and random internal crystal strains. Therefore, many attempts to observe the EPR signal of acceptor impurities in these semiconductors were unsuccessful [4–6].

The first observation of the EPR signal from the boron atom in a uniaxially stressed silicon crystal was reported in 1960 [4]. To the best of our knowledge, the only paper was published where EPR spectra of boron atoms in silicon crystals without applied external stress were reported [7]. As was noted by the author of this paper, some phenomena had no reasonable explanations: (i) the temperature dependence (in the range from 4.2 K to 1.2 K) of the "fine" structure of the EPR spectra; (ii) decrease of the signal amplitude with decreasing thickness of the samples and (iii) two-fold broadening of the line after finely grinding the samples.

The present paper contains the results on behaviour of residual polarization of negative muons in silicon doped with phosphorus and antimony, as well as in graphite, germanium and copper. The impurity concentrations in phosphorus and antimony doped silicon samples were $[P]=1.6\cdot10^{13}$ cm^{-3} and $[Sb]=2\cdot10^{18}$ cm^{-3} respectively. A graphite sample served as a reference to determine muon beam polarization and parameters of the installation under the working conditions. The measurements in germanium were carried out to verify the total loss of negative muon polarization observed in [8] under unfavorable conditions. The total loss of polarization would have excluded any further μ^-SR investigations in germanium in transverse magnetic fields.

1. Experimental setup

The measurements were performed on the "Stuttgart LFQ Spectrometer" [9] in the μE4 beam channel of the PSI accelerator. The magnetic field of 0.1 T was produced by Helmholtz coils transverse to muon spin polarization. The target thickness along the beam direction was 2.6, 3.8, 2.4, 2.1 g/cm^2 for the phosphorus doped silicon, antimony doped silicon, graphite and germanium samples respectively. The samples had an approximately equal area about 7 cm^2. To cool the target vapor flow of liquid helium was used. The temperature of the target was stabilized with an accuracy of 0.1 K. The spectrometer time bin was 0.625 ns, the total number of channels in the spectrum was 16000. Electrons from stopped muons were registered by counters placed in front of and behind the target. Thus, two spectra from the decay electrons, moving forward (FW) and backward (BW) relative to the muon beam direction, were stored simultaneously. The muon stop rate in the target was about 10^4 per second. The beam momentum adjusted for the best effect-to-background ratio was 60 MeV/c.

2. Results

Besides the target some of muons stop in the cryostat walls and in the scintillation counters and contribute to the spectrum. Since the negative muon lifetime in the 1S-state depends on the nuclear charge, the time distribution of electrons from the $\mu^- \to e^-$ decay can be given as:

$$f(t) = \sum_x N_x e^{-t/\tau_x} [1 + \alpha p_x(t)] + B(t), \quad (1)$$

where $N_x, \tau_x, p_x(t)$ are respectively the preexponential multiplier, the

muon lifetime and the projection of the muon polarization onto the observation direction for the chemical element X, α is the asymmetry coefficient in the space distribution of decay electrons assuming the registration solid angle, B is the background of accidental coincidences.

The background was modulated with the frequency $\nu_{hf} = 50.6328$ MHz due to the proton beam microstructure. It was found from the preliminary Fourier analysis that the spectra contained higher harmonics of ν_{hf} as well. As a result, B was presented as ($\omega_{hf} = 2\pi\nu_{hf}$):

$$B = b_0 + \sum_{n=1}^{2} b_n \cos(n\omega_{hf} t + \phi_n). \quad (2)$$

The experimental data were fitted by the least square method. The negative muon lifetimes were fixed at the mean values of the experimental data given in [10] (2030 ns, 760 ns, 167 ns and 163 ns for carbon, silicon, germanium and copper, respectively).

I. Copper

To determine $p_{Cu}(t)$ a measurement with a copper sample was carried out. The measurement was necessary for correct consideration of the copper contribution in processing of the experimental data for different samples. In this case the spectra contained two components with the negative muon lifetimes τ_C in carbon and τ_{Cu} in copper. Since copper atoms have got nonzero nuclear spin, there is additional depolarization of the muon caused by hyperfine interaction between the magnetic moments of the nucleus and muon [11, 12]. Analysis of the data shows that $a_\pm$, the amplitudes of the muon spin precession at frequencies $\omega_\pm = \gamma_\pm H$ corresponding to the hyperfine states with total moments $F_\pm = I \pm S_\mu$, are equal to zero within experimental errors: $a_\pm = (0.2 \pm 0.3)\%$. The present result agrees with the data from [13, 14].

From the experimental data on copper and germanium the polarization function $p_C(t)$ corresponding to muons stopped in the scintillation counters was obtained. The contribution from counters depends on the sample thickness and appears to be 7%, 4% and 1.5% for copper, silicon and germanium samples respectively (for the "forward" spectrum). The contribution is well described by the function $p_C(t) = p_0 \cos(\omega t + \phi)$, of muons stopped in the cryostat walls depends only on the effective stopping thickness of the target. To determine the dependence of the copper contribution on the target thickness the appropriate measurements in silicon were carried out.

After correction to the copper contribution, $a = \alpha p_0$ in germanium was found to be (2.2± 0.2)%, (2.4±0.2)%, (2.3±0.2)% and (2.7±0.2)% at 4.5 K, 30 K, 100 K and 290 K respectively.

Systematic errors, which arise from the correction for the copper contribution, were not taken into account. It follows from the presented data that muon polarization in the 1S-state of germanium is only 30–40% less than in carbon. Probably, there is a slight decrease in the polarization with decreasing temperature. Muon spin relaxation in germanium within errors was not observed. Averaged over 4.5 K, 30 K, 100 K and 300 K, the muon spin precession frequency for the germanium sample is 84.9 ± 0.4 rad/μs.

IV. Phosphorus doped silicon

The silicon sample spectrum contains contributions from copper, silicon and carbon. Accordingly, the function describing the experimental data, besides background, contains three terms. Considering muon spin relaxation at low temperatures, the polarization function for silicon was expressed as:

$$p(t) = p_0 e^{-\lambda t} \cos(\omega t + \phi), \quad (3)$$

where λ is the muon spin relaxation rate. The functions for the copper and carbon contributions were presented above.

Examples of μ^-SR spectra for the phosphorus doped silicon sample are shown on fig. 2. The background, copper and carbon contributions are subtracted. For visual presentation the data are multiplied by $\exp(t/\tau_{Si})$. It is clearly seen that muon spin relaxation takes place at low temperatures.

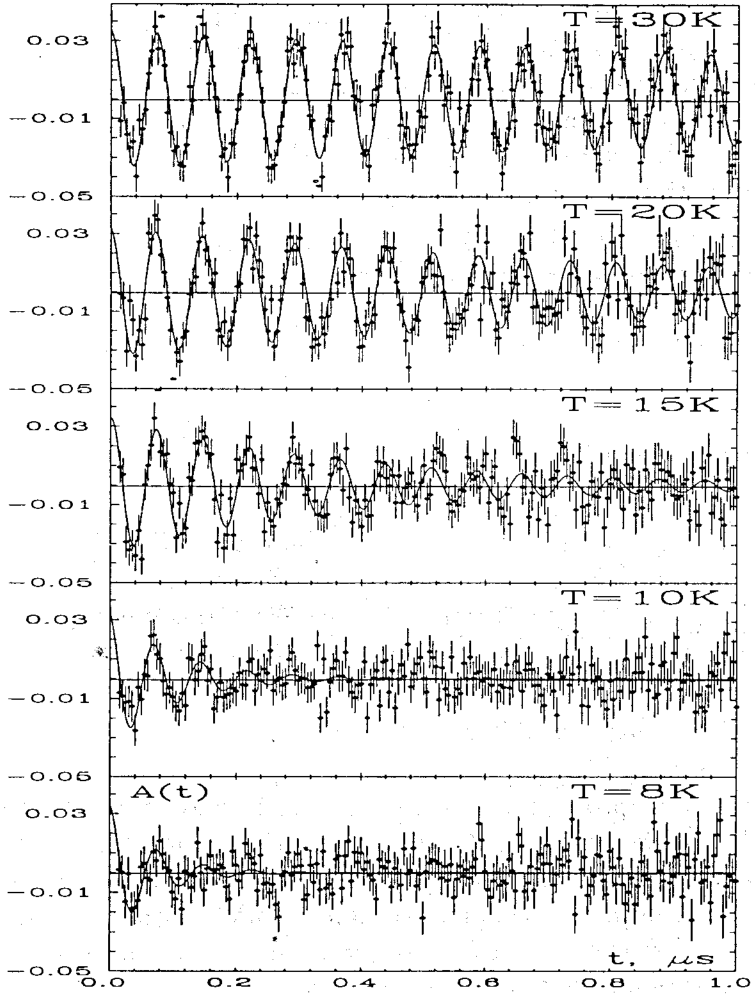

Figure 2: Phosphorus doped silicon sample. μ^-SR spectra after background subtraction and correction for the negative muon lifetime.

where $\alpha p_0 = 0.009 \pm 0.002$. For further analysis it was accepted that $p_{Cu}(t) = 0$ and $\alpha p_C = 0.009\cos(\omega t + \phi)$.

II. Graphite

In the processing of the graphite sample data, the copper contribution was taken into account. It was accepted that $p(t) = p_0\cos(\omega t + \phi)$ for graphite.

Table 1 presents the muon spin precession amplitude $a = \alpha p_0$ and frequency determined for the graphite sample from "backward" (BW) and "forward" (FW) spectra at different temperatures.

As follows from table 1, a is constant in the range 4 K–300 K within the errors. This could be explained by high conductivity of graphite in the temperature range. The difference in the precession amplitudes for the FW and BW spectra by 7.5% is caused by the setup geometry.

As is seen, $\delta\omega/\omega$ for a single measurement is approximately equal to $2{\cdot}10^{-4}$. A dispersion relative to the averaged value is less than an error for a single measurement. This means that the precision of ω is limited by the statistics. Therefore, the stability of the external magnetic field was not worse than $2{\cdot}10^{-4}$ and the spectrometer allows one to measure the frequency with the same accuracy.

Table 1: The muon spin precession amplitude and frequency determined for the graphite sample at different temperatures from "forward" (FW) and "backward" (BW) spectra.

T,K	ω (FW), rad/μs	ω (BW), rad/μs	a (FW), %	a (BW), %
4	85.112±0.017	85.102±0.020	3.70±0.09	4.14±0.10
20	85.135±0.018	85.121±0.022	3.75±0.10	4.20±0.11
300	85.083±0.017	85.128±0.021	3.55±0.09	4.14±0.11
averaged	85.113±0.008		3.65±0.06	4.16±0.07

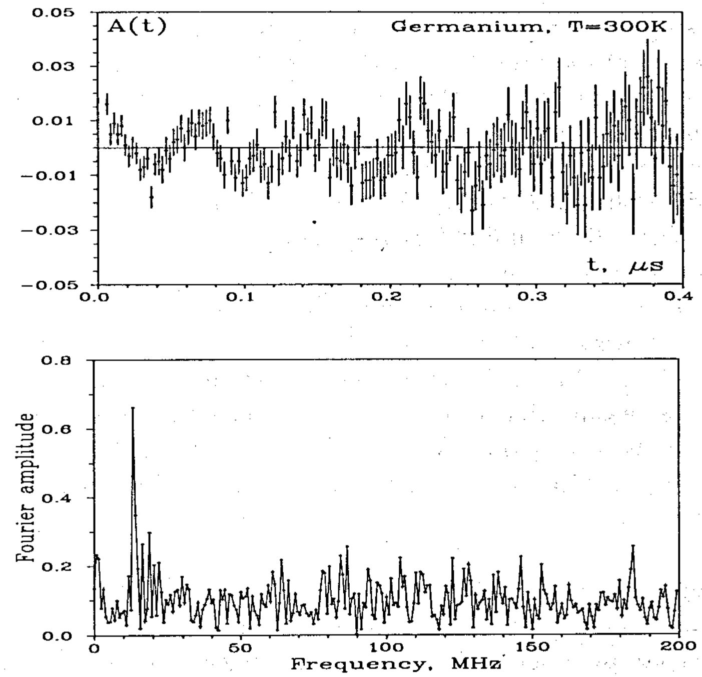

Figure 1: An example of the μ^-SR spectrum for the germanium sample after background subtraction and correction for the negative muon lifetime at T = 300 K. The lower picture is its Fourier image.

III. Germanium

The negative muon lifetimes in germanium and copper are close. For this reason the contributions from the sample and the cryostat walls were described by a single exponential term in (1), the lifetime being considered as a free parameter.

Figure 1 shows an example of the μ^-SR spectrum for the germanium sample at 300 K. The precession frequency is equal to the free muon spin frequency within errors and corresponds to the peak on the Fourier image of the spectrum.

It was assumed that muons captured by copper atoms are totally depolarized within a time inaccessible to observation and that the fraction

Figure 3 gives the temperature dependence of the relaxation rate and precession frequency shift $\delta\omega/\omega_0$, where ω_0 is the precession frequency at room temperature. The temperature dependence of the relaxation rate is well approximated by the function $\lambda = d \cdot T^{-q}$, where $d = (4.0 \pm 0.7) \cdot 10^3\ \mu s^{-1}$, $q = 2.73 \pm 0.06$, the temperature is given in Kelvins. In the present study the value of the parameter q was found four times more precisely than in the previous works [2, 3]. The data given in Fig.3 confirm the conclusion [3] that at $T < 30$ K there is a shift of the muon spin precession frequency. The accuracy of the $\delta\omega/\omega_0$ measurements is two times better as compared with [3].

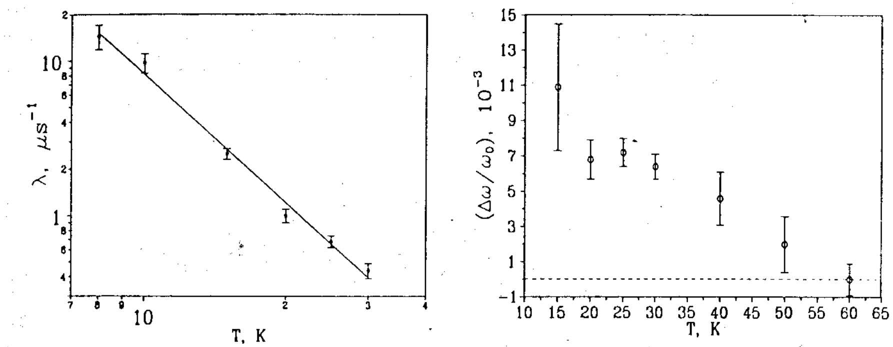

Figure 3: Phosporus doped silicon sample. The temperature dependencies of the relaxation rate and frequency shift. ($\omega_0 = 84.89 \pm 0.04$ rad/μs)

V. Antimony doped silicon

Preliminary data processing showed that polarization function (3) was not suitable for describing the low temperature experimental data for the antimony doped silicon sample. After correction to the muon lifetime the presence of both damped and undamped polarization components in the spectra is evident (see fig.4). The term "undamped" means that the possible relaxation rate does not exceed 0.05 μs^{-1}.

Therefore, for further data processing the polarization function $p(t)$ was taken as:

$$\alpha p(t) = a_1 e^{-\lambda t} \cos(\omega_1 t + \phi_1) + a_2 \cos(\omega_2 t + \phi_2) \qquad (4)$$

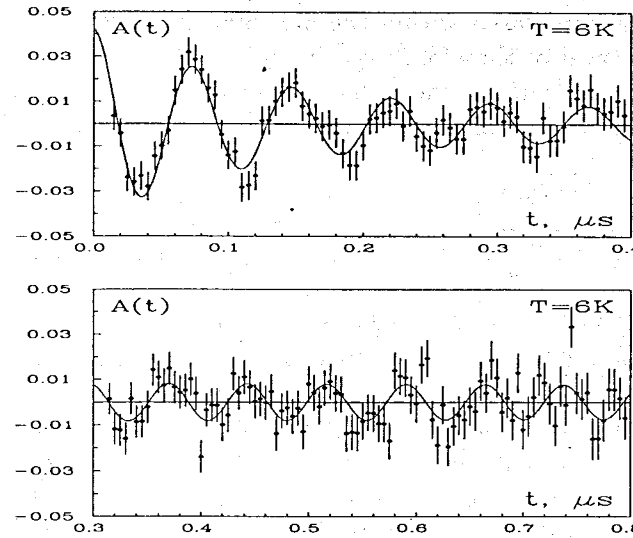

Figure 4: Antimony doped silicon sample. μ^-SR spectrum at 6 K in different time windows.

To test the reliability of the results obtained by using polarization function (4) for the expected values $(a_1 + a_2) \leq 0.05$ computer simulations were done. Two spectra with the statistics close to the experimental one were simulated with a random number generator. Like the experimental data, the simulated spectra had three constituents with parameters describing muon decay in the 1S-state of copper, carbon and silicon. The muon polarization function for the silicon constituent was given as (4) with various a_1 and a_2. The ratios N_{Cu}:N_C:N_{Si}:B were taken from the real spectra. In the model spectra there were 1900 channels, each 5 ns wide, which corresponded to the time interval 9.5 μs. Table 2 presents the values of the parameters used in the simulation and obtained after processing the simulated spectra by the least square method. For the spectrum simulated with $a_2 = 0$ the processing gives a_2 close to zero within the error estimation. For the spectrum simulated with the parameters $a_1 = 2.8$ % and $a_2 = 0.6$% good agreement was obtained with the fitted values of the parameters. The fit of the second spectrum with fixed $a_2 = 0$ leads to an increase in χ^2. It should be noted that all the difference in χ^2 is accumulated within the first 500 channels of the spectrum – the time interval of threefold negative muon lifetime in silicon. Thus, the numerical experiments show that the separation of the damped and undamped components of polarization could be successfully solved.

Table 2: Fit results for the simulated spectra.

	Spectrum 1				Spectrum 2			
	a_1, %	a_2, %	λ, μs^{-1}	χ^2	a_1, %	a_2, %	λ, μs^{-1}	χ^2
	3.4	0	2.5		2.8	0.6	8	
Fit 1	3.2±0.2		2.3±0.3	1865	2.3±0.3		2.7±0.5	1970
Fit 2	3.1±0.3	0.1±0.2	2.6±0.5	1864	3.0±0.6	0.6±0.1	9.8±2.7	1925

The behaviour of negative muon polarization in this sample considerably differs from that in the other investigated silicon samples with different impurity types and concentrations [1–3]. The function describing muon spin polarization contains both damped and undamped components. It was found that the sum of the amplitudes of the components $(a_1 + a_2)$ is independent of temperature within the experimental errors and equal to the muon spin precession amplitude observed at room temperature. The temperature dependence of a_1 and a_2 is shown in fig. 5.

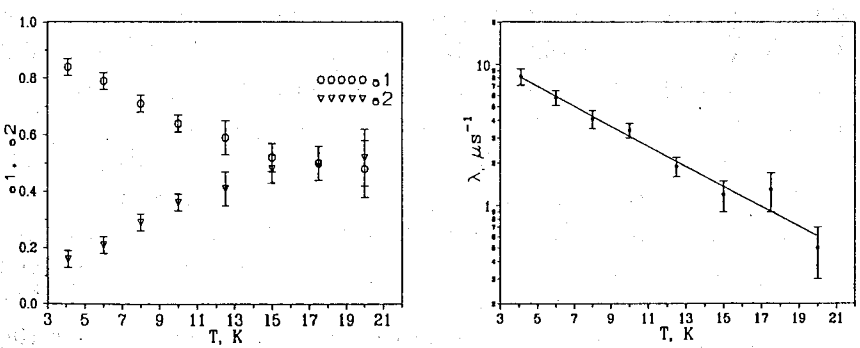

Figure 5: Antimony doped silicon sample. The temperature dependence of the relative amplitudes of the damped ($a1$) and undamped ($a2$) components of the negative muon polarization ($a1 + a2 = 1$). The temperature dependence of the relaxation rate.

The amplitude of the damped component (a_1) at 4.1 K is about 85% of the sum. With increasing temperature, a_1 decreases and at 17 K $a_1 \approx a_2$. The rapid decrease in the component relaxation rate with increasing temperature (fig. 5) makes it impossible to identify the components at $T \geq 27$ K. The processing of the experimental data obtained at 40 K shows the absence of a damped component with relaxation rate $\lambda \geq 5 \cdot 10^4$ s^{-1} in the spectrum. The temperature dependence of the relaxation rate is weaker than in the samples investigated earlier and is better described by the exponential rather than power dependence, though the latter cannot be excluded. Using the relation $\lambda = \eta \cdot e^{-\beta T}$ to describe the data we obtained the following values for the parameters: $\eta = (16 \pm 2)$ μs^{-1}, $\beta = (0.167 \pm 0.014)$ K^{-1} (see fig. 5). The muon spin precession frequencies for the damped and undamped components differ from each other. For the undamped component it corresponds to the free muon spin precession frequency whereas for the damped component a frequency shift is observed at temperatures lower than 20 K. The mean value of the frequency shift $\delta\omega/\omega$ in the temperature range 8 – 20 K is $(8.0\pm2.2)\cdot10^{-3}$.

3. Discussion

Observation of the damped and undamped components in the residual polarization of negative muons indicates that during the observation time the acceptor center can be found both in the ionized $_\mu$Al$^-$ and neutral $_\mu$Al^0 states. Therefore, it is necessary to assume that either muonic atoms are originally (for the time less than $1/\Omega_{hf}$) formed both in the ionized and neutral states or there is a transition between the states with a rate comparable to $1/\tau_{Si}$.

In this case the behaviour of the complex polarization ($\mathbf{p} = p_x + ip_y$) in the transverse magnetic field ($H \parallel z$) is described by the following system of differential equations:

$$\frac{d}{dt}\begin{pmatrix} \mathbf{p}_1 \\ \mathbf{p}_2 \end{pmatrix} = \begin{pmatrix} -(\lambda + \nu_{12}) + i\omega_1 & \nu_{21} \\ \nu_{12} & -\nu_{21} + i\omega_2 \end{pmatrix} \begin{pmatrix} \mathbf{p}_1 \\ \mathbf{p}_2 \end{pmatrix}, \quad (5)$$

where indices 1 and 2 denote neutral (paramagnetic) and ionized (diamagnetic) states of the acceptor center respectively. The experimentally observed value is p_x=Re $\mathbf{p}$, where $\mathbf{p}$ is the total polarization $\mathbf{p}_1$+$\mathbf{p}_2$.

The solution of the system of differential equations (5) contains the undamped component if $\nu_{21} = 0$. Under the initial condition $p(0) = 1$ the solution can be presented as ($\delta = \omega_1 - \omega_2$, $\nu = \nu_{12}$):

$$p_x(t) = C_1 e^{-(\lambda+\nu)t}\cos(\omega_1 t + \varphi_1) + C_2\cos(\omega_2 t + \varphi_2),$$

$$C_1 = \frac{n_1\sqrt{\lambda^2+\delta^2}}{\sqrt{(\lambda+\nu)^2+\delta^2}}, \qquad C_2 = \frac{\sqrt{(n_2\lambda+\nu)^2+(n_2\delta)^2}}{\sqrt{(\lambda+\nu)^2+\delta^2}}, \qquad (6)$$

$$\tan\varphi_1 = -\frac{\nu\delta}{\lambda(\lambda+\nu)+\delta^2}, \quad \tan\varphi_2 = \frac{n_1\nu\delta}{(n_2\lambda+\nu)(\lambda+\nu)+n_2\delta^2},$$

where n_1 and n_2 are the initial populations of states 1 and 2 respectively, $n_1 + n_2 = 1$.

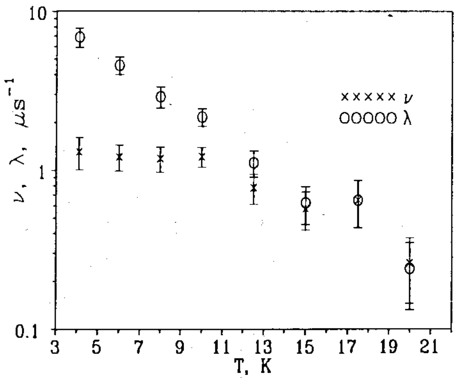

Figure 6: The temperature dependencies of the muon spin relaxation λ and transition $(1 \rightarrow 2)$ ν rates for the antimony doped silicon sample.

As is seen, besides the trivial case $\nu = 0$, when any transitions between states are absent and the relation between amplitudes is equal to that of initial populations, it is possible to observe the undamped component even if state 2 is initially completely unpopulated ($n_2 = 0$).

The results of the fit (under the condition $n_2 = 0$) of the experimental data for the antimony doped silicon sample using two-component polarization function (6) are shown in Fig.6. As is seen, the transition

rate is practically constant in the temperature range 4 K–12 K and approximately equal to $1.2 \cdot 10^6$ s^{-1}. Over 13 K the transition rate begins decreasing with increasing temperature.

Muon spin relaxation at a frequency close to that of free muon spin is due to relaxation of the magnetic moment of the electron shell of the muonic atom, which is the acceptor impurity in semiconductors. In the hydrogen-like atom approximation, which is often used for describing an (acceptor center + hole) system, the relaxation rate of the muon spin can be expressed as [18]:

$$\lambda = \Omega_{\rm hf}^2/4\nu_{\rm r}, \qquad (7)$$

where $\nu_{\rm r}$ is the relaxation rate of the magnetic moment of the electron shell of the acceptor center, $\Omega_{\rm hf}^2$ is the frequency of hyperfine interaction between the magnetic moments of the muon and the electron shell of the acceptor center.

Using the value $\Omega_{\rm hf}/2\pi = 650$ MHz from [15] and the value λ obtained for phosphorus doped silicon, we found that $\nu_{\rm r} = 1.6 \cdot 10^{12}$ s^{-1} at $T = 15$ K. Extrapolated according to the dependence $\lambda = d \cdot T^{-q}$ to 4 K the value of λ leads to $\nu_{\rm r} = 5 \cdot 10^{10}$ s^{-1}. This value does not contradict the results of the EPR measurements carried out in a silicon crystal under uniaxial stress [5].

As shown in [16, 17], the following processes can give a contribution to spin-lattice relaxation of shallow acceptor centers in silicon: the direct (one-phonon) process, the Raman process, and the resonance fluorescence (the Orbach process). At temperatures below 1 K the one-phonon process dominates, at intermediate temperatures the Raman scattering does, and at high temperatures the resonance fluorescence takes place. However, the temperature at which the resonance fluorescence contribution exceeds that of the Raman scattering is argued [16, 17] and is in the temperature range 10 – 100 K. The spin-lattice relaxation rate is proportional to T for the one-phonon process, to T^5 (T^7) for the Raman scattering, and to $\exp(-\Delta/T)$ for the resonance fluorescence. It is obvious that for intermediate temperatures, when the contributions of different processes are comparable, the temperature dependence of spin-lattice relaxation becomes more complicated.

From the observed temperature dependence of the muon spin relaxation one can conclude that the one-phonon process hardly contributes to the relaxation of the magnetic moment of the acceptor center in the temperature range 4 – 40 K.

It follows from the preliminary estimations that acceptor-donor pair formation and recombination of charge carriers and excitons on this pair are probably the main cause of the undamped component in muon polarization for the antimony doped silicon sample. If this idea is right, the μSR method can be used to study kinetics of charge carrier recombination on an isolated acceptor center in semiconductors.

Acknowledgments

Authors are grateful to Dr. V.G Firsov for providing the silicon samples.

References

[1] T.N.Mamedov, V.N.Duginov, V.G.Grebinnik et.al., Hyp. Int. 86, 717 (1994).

[2] W.Beez, T.Grund, M.Hampele et.al., PSI Newsletter, Annex I, 125 (1993).

[3] T.N.Mamedov, I.L.Chaplygin, V.N.Duginov et.al., Hyp. Int. 105, 345 (1997).

[4] G.Feher, J.C.Hensel, E.A.Gere, Phys. Rev. Lett. 5, n.7, 309 (1960).

[5] G.W.Ludwig, H.H.Woodbury, Bull. Am. Phys. Soc. 6, 118 (1961).

[6] T.Shimizu, N.Tanaka, Phys. Lett. 45A, n.1, 5 (1973).

[7] H.Neubrand, phys. stat. sol. (b) 86, 209 (1978).

[8] Th.Stammler, R.Abela, Th.Grund et.al., phys. stat. sol. (a) 137, 381 (1993).

[9] R.Scheuermann, J.Schmidl, A.Seeger, Th.Stammler, D.Herlach, J.Major, Hyp. Int. 106, 295 (1997).

[10] T.Suzuki, D.F.Measday, J.P.Roalsvig, Phys. Rev. C35, 2212 (1987).

[11] A.P.Buhvostov, Yadernaya Physika 9, n.1, 107 (1969).

[12] H.Überall, Phys. Rev. 114, 1640 (1959).

[13] V.S.Evseev, A.I.Klimov, T.N.Mamedov et.al., preprint IAE-3242/2, Moscow, 1980.

[14] J.H.Brewer, Hyp. Int. 19, 873 (1984).

[15] M.Koch, K.Maier, J.Major et.al., Hyp. Int. 65, 1039 (1990).

[16] T.Shimizu, M.Nakayama, J. Phys. Soc. Japan 19, 930 (1964).

[17] Y.Yafet, J. Phys. Chem. Solids 26, 647 (1965).

[18] V.N.Gorelkin, D.V.Rubtsov, Hyp. Int. 105, 315 (1997).

**Received by Publishing Department
on April 29, 1998.**